

1
2
3
4
5
6
7
8
9
10
11

Supplementary Information

Delivery of exogenous mitochondria via centrifugation enhances cellular metabolic function

Mi Jin Kim¹, Jung Wook Hwang¹, Chang-Koo Yun¹, Youngjun Lee², Yong-Soo Choi^{1*}

¹Department of Biotechnology, CHA University, Seongnam, 13488, Republic of Korea

²Paeon Biotechnology Inc., Daejeon, 34028, Republic of Korea

12 **Supplementary Methods**

13

14 **Isolation of mitochondria**

15 Mitochondria were isolated from donor cells by differential centrifugation. The experimental flow chart for mitochondrial isolation is shown in
16 [Fig. S1A](#). In brief, mitochondria were prepared from 2×10^7 UC-MSCs. Cells were harvested from culture flasks, and pellets were homogenised
17 using a disposable 1 ml syringe in SHE buffer [0.25 M sucrose, 20 mM HEPES (pH 7.4), 2 mM EGTA, 10 mM KCl, 1.5 mM MgCl₂ and 0.1%
18 defatted bovine serum albumin (BSA)] containing a protease inhibitor (Roche Diagnostics, Mannheim, Germany) and centrifuged at 1,100 x g
19 for 3 min at 4°C (to remove unbroken cells and cell debris). The supernatant was then centrifuged at 12,000 x g for 15 min at 4°C to pellet
20 mitochondria. The mitochondrial pellet was resuspended in 500 µl of SHE buffer and centrifuged at 20,000 x g for 10 min at 4°C, after which
21 the supernatant was removed. The pellet was resuspended and centrifuged at 20,000 x g for 5 min at 4°C. After removal of the supernatant, the
22 pellet was resuspended in 50 µl of PBS and kept on ice until measurements were performed. Isolated mitochondria were quantified by determining
23 the protein concentration using a bicinchoninic acid assay (Pierce, Rockford, IL). All assays were performed with freshly isolated mitochondria.

24

25 **Labelling of mitochondria**

26 To visualise mitochondrial transfer, cells were separately labelled 24 h before mitochondrial isolation and transfer with MitoTracker Green FM
27 or MitoTracker Red CMXRos (Molecular Probes, Invitrogen, Carlsbad, CA) according to the manufacturer's protocol. Briefly, cells were
28 resuspended in prewarmed (37°C) staining solution containing the MitoTracker probe (300 nM) and incubated for 30 min under appropriate
29 growth conditions. After staining, cells were washed thrice with phosphate-buffered saline (PBS) and resuspended in fresh prewarmed medium.
30 The cells were harvested or plated according to the experiment.

31

32 **Transmission electron microscopy**

33 Isolated mitochondria (100 µg) were fixed with 2% paraformaldehyde and 2% glutaraldehyde (Electron Microscopy Sciences, Hatfield, PA) in
34 0.1 M cacodylate buffer (Electron Microscopy Sciences). The fixed samples were dehydrated through a series of ethanol and embedded in epoxy
35 resin (Epon 812; Sigma-Aldrich, USA). Ultrathin sections (70 nm) were cut from the resin blocks by using a diamond knife mounted on an
36 Ultracut (Leica, Tokyo, Japan). The sections were placed on copper grids, counter-stained with 2% uranyl acetate (Merck), and photographed

37 with transmission electron microscope (H-7650; Hitachi, Japan).

38

39 **Cell preparation**

40 Human adipose-derived mesenchymal stem cells (AD-MSCs; PCS-500-011, passage #7), a human breast cancer cell line (MCF-7; HTB-22,
41 passage #20), human adenocarcinoma alveolar epithelial cells (A549; CCL-185, passage #20), a human leukemic cell line (K562; CCL-243,
42 passage #20), a human hepatic cell line (WRL-68; CL-48, passage #9), human dermal fibroblasts (HDFs; PCS-201-012, passage #9) and a human
43 natural killer cell line (NK-92; CRL-2407, passage #10) were purchased from the Animal Type Culture Collection (Manassas, VA). Human bone
44 marrow-derived mesenchymal stem cells (BM-MSCs; MSC-001F, passage #7) were purchased from Stem Cell Inc. (Vancouver, Canada). To
45 compare the transfer efficiency (%) according to the cell type (Figure 2d), all cell lines were incubated in a 37°C bath until completely thawed
46 and then used immediately for mitochondrial transfer. The protocol for mitochondrial transfer is described in the Materials and Methods section.

47

48 **Measurement of reactive oxygen species (ROS) using 2',7'-dichlorofluorescein diacetate (DCF-DA)**

49 The fluorogenic substrate DCF-DA (Invitrogen) is a cell-permeable dye that is oxidised to highly fluorescent 2',7'-dichlorofluorescein by H₂O₂
50 and can therefore be used to monitor intracellular generation of ROS. To measure ROS, cells were seeded into 24-well plates after mitochondrial
51 transfer. After 48 h, cells were washed twice with PBS and incubated with 10 µM DCF-DA for 30 min. Intracellular ROS generation was
52 determined using a fluorescence ELISA reader at an excitation wavelength of 485 nm and an emission wavelength of 535 nm (Molecular Devices).

53

54 **Generation of Rho⁰ cells**

55 To generate UC-Rho⁰ cells, UC-MSCs were treated with 200 ng/ml EtBr for 6 weeks. UC-Rho⁰ cells were maintained in α-MEM supplemented
56 with 10% FBS, 1% P/S, 0.1 mM non-essential amino acids, 1 mM sodium pyruvate and 50 µg/ml uridine (Sigma-Aldrich, St. Louis, MO).
57 Specific supplements, such as pyruvate and uridine, were required to maintain their viability. The medium was changed every 2 days. The cells
58 were used at passage #8–9 for further experiments. All cell lines were maintained at 37°C in 5% CO₂.

59

60 **Induction of muscle atrophy**

61 To induce muscle atrophy, L6 muscle cells were seeded in six-well culture plate (SPL; 2 x10⁵ cells/well). And then cells were treated with 1 µM
62 Dexa (Sigma-Aldrich) in a time-dependent manner (6, 12 and 24 h) as an in vitro model for muscle atrophy. After 24 h, cells were washed twice

63 with PBS and analyzed ATP content and mROS generation ([Fig. S6A and B](#)). Based on these results, prepared mitochondria were transferred to
64 L6 cells treated with 1 μ M Dexa to investigate the changes of intracellular function ([Fig. 4](#)).

65 **Supplementary Results**

66

67 **Evaluation of the effect of mitochondrial transfer on normal cells.** To assay the generation of intracellular ROS in UC-MSCs we used two
68 fluorescent indicators (DCF-DA and MitoSOX) (Fig. S3A). DCF-DA is one of the most widely used probe for detecting intracellular H₂O₂ and
69 oxidative stress. Oxidation by ROS yields DCF, which emits green fluorescence upon excitation at 494 nm¹. Similarly, MitoSOX Red has been
70 used to measure cellular and mitochondrial superoxide formation¹. Using H₂O₂ -treated UC-MSCs as positive controls, cellular ROS production
71 was not detected in UC-MSCs 48 h after mitochondrial transfer (Fig. S3A). In addition, the intracellular ATP content at 48 h was significantly
72 increased in proportion to the amount of the mitochondria transferred (1.38-fold, 1.69-fold and 1.96-fold using 0.05, 0.5 and 5 µg of mitochondria,
73 respectively) (Fig. S3B). However, unexpectedly, no significant effect on cell proliferation was observed despite an increase in ATP content and
74 absence of ROS production (Fig. S3C).

75 Under normal physiological condition, cytochrome c is located in the mitochondrial intermembrane space. However, as mitochondrial ROS
76 production increases, cytochrome c is translocated to the cytosol, which is a key step in the apoptotic process^{2,3}. We evaluated the cytosolic
77 cytochrome c content after mitochondrial transfer by immunoblotting (Fig. S3D). After 48 h after mitochondrial transfer, cytochrome c was not
78 released into the cytosol of UC-MSCs (Fig. S3D). All in all, mitochondrial transfer by centrifugation does not lead to increased ROS production
79 or the release of cytochrome c into the cytosol (Fig. S3A).

80 In addition, we examined changes in the expression of various markers that are important for regulating mitochondrial biogenesis⁴,
81 mitochondrial dynamics [mitofusin 2 (Mfn-2) and dynamin-1-like protein (DRP-1)] and degradation [PTEN-induced kinase 1 (PINK-1) and
82 LC3B]. Unlike expectations, the expression of these markers were not observed at 48 h after mitochondrial transfer (Fig. S3E), suggesting that
83 it is necessary to track changes of these markers at different time points.

84 Finally, the metabolic activity of UC-MSCs after mitochondrial transfer was investigated. Compared to normal UC-MSCs, mitochondrial transfer
85 effectively improved oxygen consumption of the basal and maximal OCR, respectively (Fig. S3F, G and H). Also, increases in OCR were
86 observed in ATP production and spare respiratory capacity after mitochondrial transfer (Fig. S3G, I and J). Importantly, the spare respiratory
87 capacity, a major factor determining cell survival, increased proportionately to the amount of mitochondria transferred (Fig. S3J), indicating that
88 exogenous mitochondria can modify the metabolic activity of UC-MSCs by regulating their respiratory capacity.

89 **Supplementary Figure Legends**

90

91 **Supplementary Figure S1. Isolation of mitochondria from UC-MSCs.**

92 (A) Schematic of the steps used to isolate mitochondria from UC-MSCs. (B–D) Confocal microscopy images of isolated mitochondria showing
93 that their membrane potential was maintained. (B) Endogenous mitochondria of UC-MSCs were counterstained with MitoTracker Green prior
94 to isolation. (C) Isolated mitochondria were stained with MitoTracker Red CMXRos, whose accumulation is dependent upon the MMP. (D)
95 Overlay of (B) and (C). Scale bar, 100 μm . (E) To verify the purity of mitochondria, the enrichment of intact mitochondria was confirmed by
96 immunoblot analysis of cytosolic and mitochondrial fractions using antibodies against COX IV (a mitochondrial marker), cytochrome C (a
97 mitochondrial marker), PCNA (a nuclear marker) and β -actin (a cytosolic marker). (F) Transmission electron microscopy of isolated
98 mitochondria. Scale bar, 1,000 nm. (G) The ATP contents of the specified amounts of isolated mitochondria (μg of protein) were measured by a
99 chemiluminescence assay. All values are shown as mean \pm SEM. N=3. *P < 0.05 vs. normal UC-MSCs (0 μg). The grouping of blots were
100 obtained from different gel, respectively. Full length image of results by Western blot were represented in [Fig. S7](#).

101

102 **Supplementary Figure S2. Verification of mitochondrial delivery using centrifugal force.**

103 (A) representative result showing the ratio of green fluorescence determined by flow cytometry following mitochondrial transfer (0.05 μg of
104 protein) according to the centrifugation duration (5, 10 and 15 min) and centrifugal force (500, 1,000, 1,500 and 2,000 $\times\text{g}$). After mitochondrial
105 transfer, the fluorescence signal intensity in UC-MSCs was quantified using Image J in a minimum of three independent experiments. All values
106 are mean \pm SEM. N=3. *P < 0.05 vs. normal UC-MSCs (0 μg). (B, C) Confocal microscopy images showing intracellular fluorescence of
107 transferred mitochondria (green) in rat L6 muscle cells prelabelled with a red MitoTracker. (B) A representative image prior to mitochondrial
108 transfer; MT (-). (C) A representative image after mitochondrial transfer; MT (+). Red: endogenous mitochondria of L6 cells, green: transferred
109 mitochondria of UC-MSCs, blue: nuclear staining with DAPI, yellow: merged mitochondria. Scale bar, 10 μm . (D, E) Comparison of the transfer
110 efficiency, as determined by the intensity of green fluorescence, following treatment with various amounts of PF-68 for various amounts of time.
111 (D) Representative results showing the uptake efficiency upon co-incubation at 37°C without centrifugation (D) and upon centrifugation for 5
112 min (E) following treatment of recipient cells with various concentrations of PF-68 (10, 20 and 30 mg/ml) for various amounts of time (0, 1 and
113 2 h).

114

115 **Supplementary Figure S3. Analysis of metabolic changes in normal cells after mitochondrial transfer.**

116 Various parameters of normal UC-MSCs were assessed at 48 h after transfer of various amounts of mitochondria (expressed as μg of protein).
117 Changes in intracellular ROS (A) by MitoSOX red (upper) and DCF-DA green (lower) probes, the intracellular ATP content (B) and cell
118 proliferation (C) were analysed and compared. Scale bar, 25 μm . (D) Immunoblot analysis of cytochrome c (Cyto C) in the total cell lysate of
119 UC-MSCs, and cytosolic fraction obtained from UC-MSCs after mitochondrial transfer. (E) Immunoblot analysis using antibodies against Mfn-
120 2 (a mitochondrial fusion marker), DRP-1 (a mitochondrial fission marker), PINK-1 (a mitophagy marker), microtubule-associated protein
121 1A/1B-light chain 3 (LC3B, an autophagy marker) and β -actin (a cytosolic marker). Representative western blots are shown, along with
122 quantification of the expression levels normalised to that of β -actin. (F) OXPHOS activity. OCRs (pmol/min) were measured in triplicate in three
123 experiments. The OCRs of basal respiration (G), maximal respiration (H), ATP production (I) and spare respiratory capacity (J) are shown. All
124 data represent the mean \pm SEM. N=3, *P < 0.05 vs. control (normal UC-MSCs). The grouping of blots were obtained from different parts of the
125 same gel. Full length image of results by Western blot were represented in [Fig. S7](#).

126

127 **Supplementary Figure S4. Metabolic changes in oligomycin-treated UC-MSCs after delivery of intact mitochondria.**

128 Oligomycin-treated cells were analysed at 48 h after transfer of various amounts of mitochondria (expressed as μg of protein). To induce
129 mitochondrial dysfunction, UC-MSCs were treated with 50 μM oligomycin for 24 h prior to mitochondrial transfer. Changes in cell proliferation
130 (A), the intracellular ATP content (B), the MMP (C) and mitochondrial ROS (D) were analysed and compared under serum-free conditions. (E,
131 F) Immunoblot analysis of AMPK (E) and PGC-1 α (F). Representative western blots are shown, along with quantification of the expression
132 levels normalised to that of β -actin. All data represent the mean \pm SEM. N=3, *P < 0.05 vs. oligomycin-treated group. The grouping of blots
133 were obtained from different parts of the same gel. Full length image of results by Western blot were represented in [Fig. S7](#).

134

135 **Supplementary Figure S5. Characterisation of UC-Rho⁰ cells.**

136 Analysis was performed after treatment with EtBr for 6 weeks to confirm the induction of UC-Rho⁰ cells. (A) UC-MSCs-specific mtDNA (Cord-
137 mtDNA) and human-specific mtDNA (Universal-mtDNA) were analysed by general PCR. Representative gels showing PCR analysis of h-
138 mtDNA (markers in bp) are shown, together with densitometric analysis of the amplified products. (B) Verification of universal-mtDNA deletion

139 by serial-passaging of UC-Rho⁰ cells compared to normal UC-MSCs. (C) The intracellular ATP content of UC-Rho⁰ cells was measured by a
140 chemiluminescence assay and compared with that of non-treated UC-MSCs. (D) Confocal microscopy images showing the mitochondrial
141 network in UC-MSCs and UC-Rho⁰ cells. Cells were incubated with 300 nM MitoTracker Red CMXRos for 30 min. Scale bar, 100 μm (E)
142 OXPHOS activity. OCRs (pmol/min) in UC-Rho⁰ cells were measured in triplicate in three experiments. The OCRs of basal respiration (F),
143 maximal respiration (G), ATP production (H) and spare respiratory capacity (I) are shown. All data represent the mean ± SEM of three
144 independent experiments. N=3, *P < 0.05 vs. non-treated UC-MSCs.

145

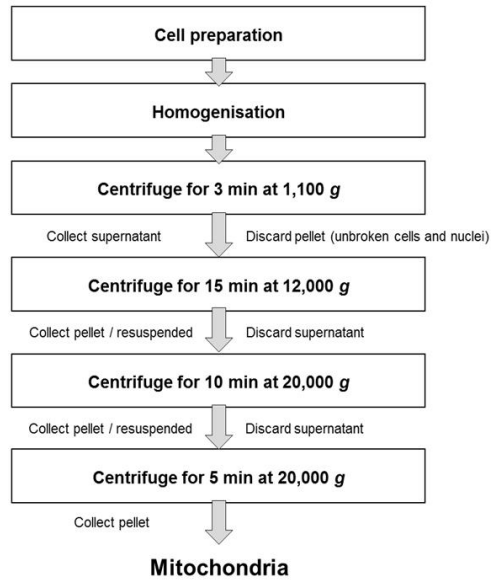
146 **Supplementary Figure S6. Verification of mitochondrial dysfunction after Dexa treatment.**

147 (A) Dexa (1 μM) treatment depleted the intracellular ATP content of L6 muscle cells in a time-dependent manner. (B) Determination of mROS
148 production following Dexa treatment for 24 h using MitoSOX Red staining. All data represent the mean ± SEM. N=3, *P < 0.05 vs. control.

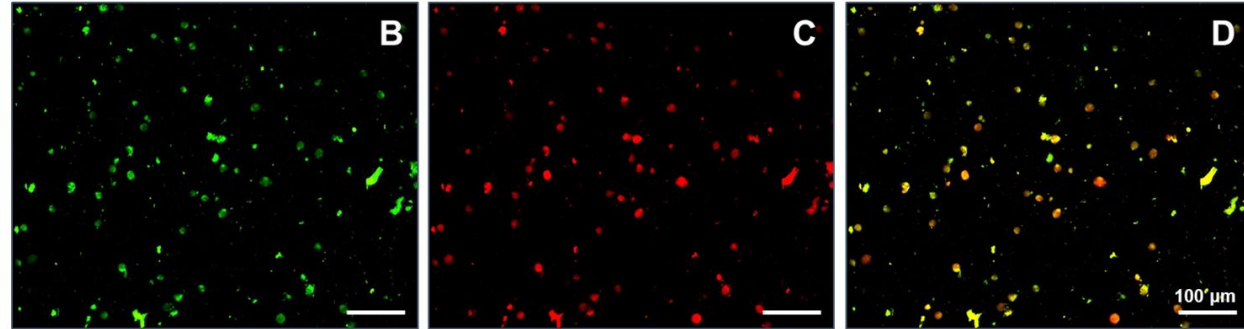
149

150

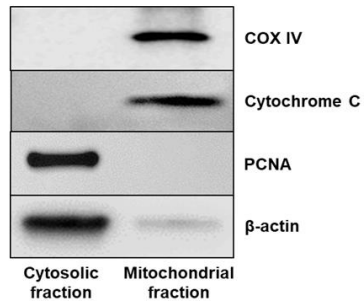
A.



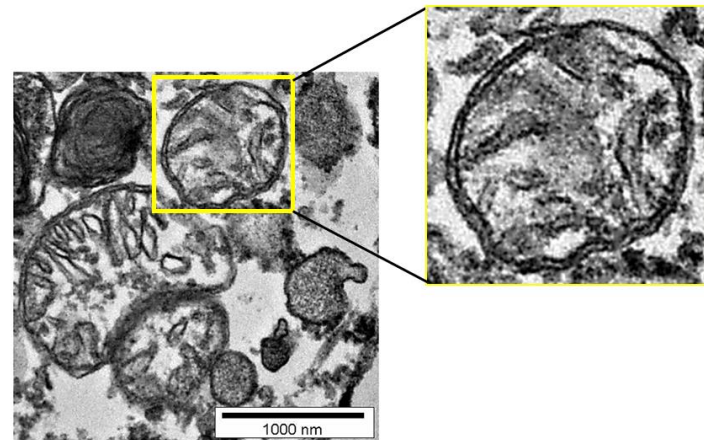
B-D



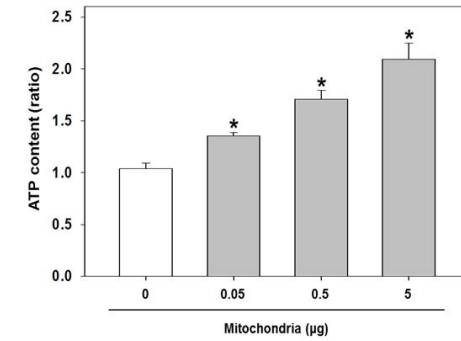
E.



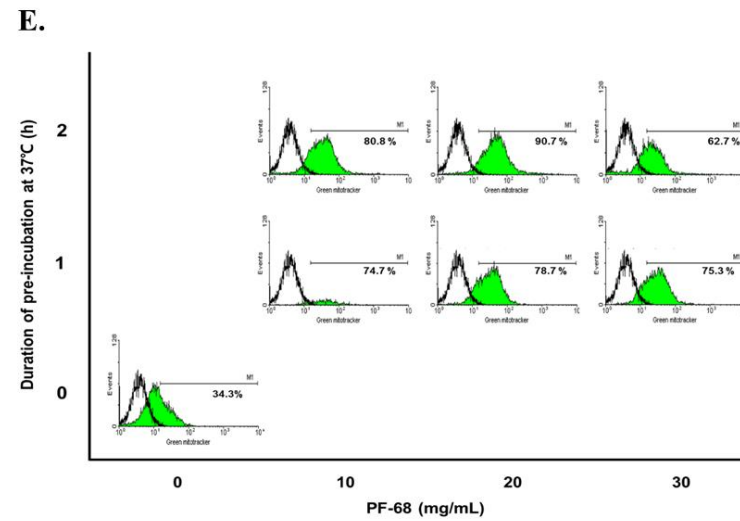
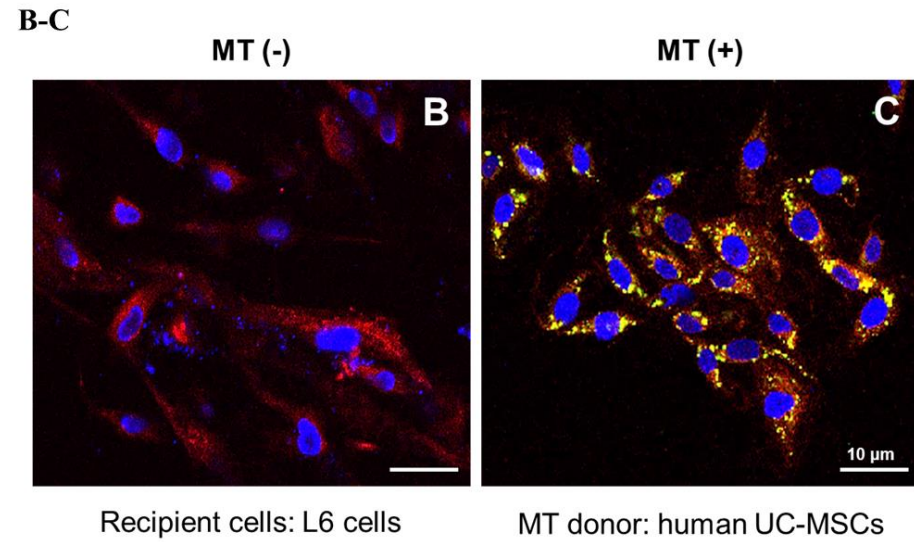
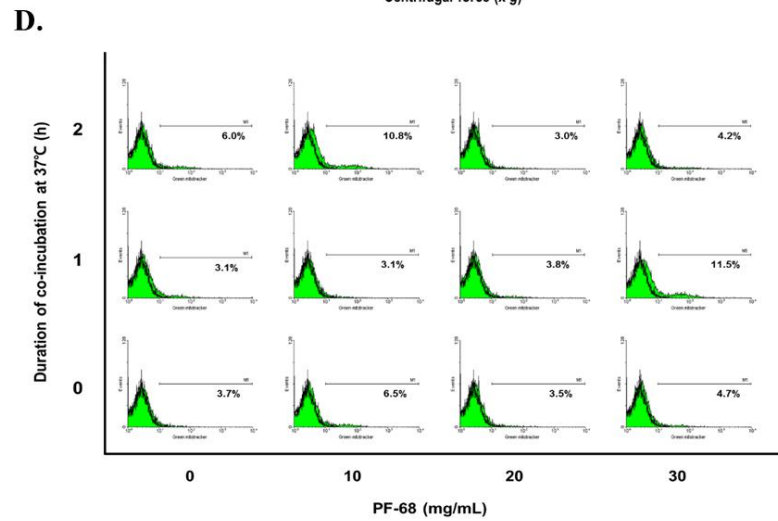
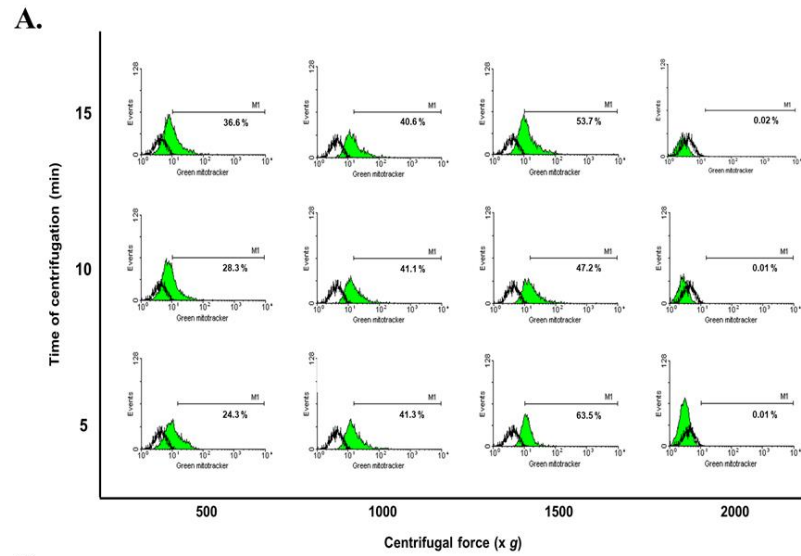
F.



G.

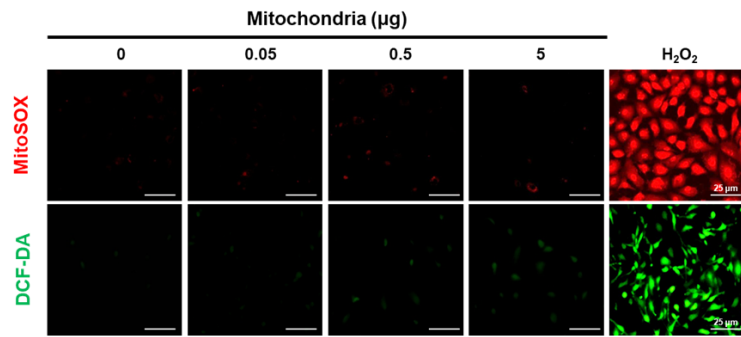


Supplementary Figure S1.

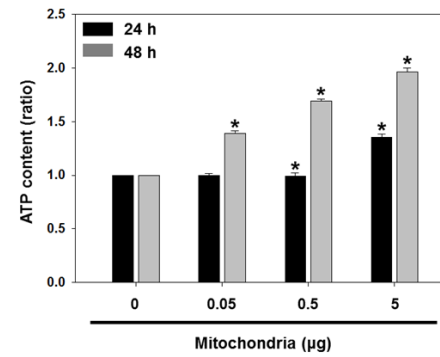


Supplementary Figure S2

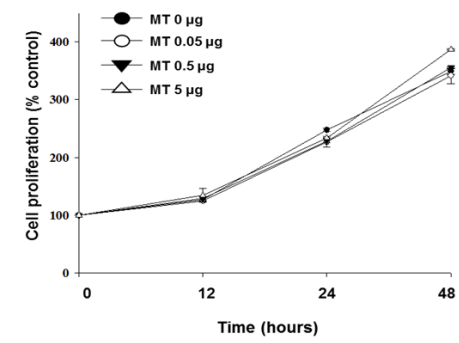
A.



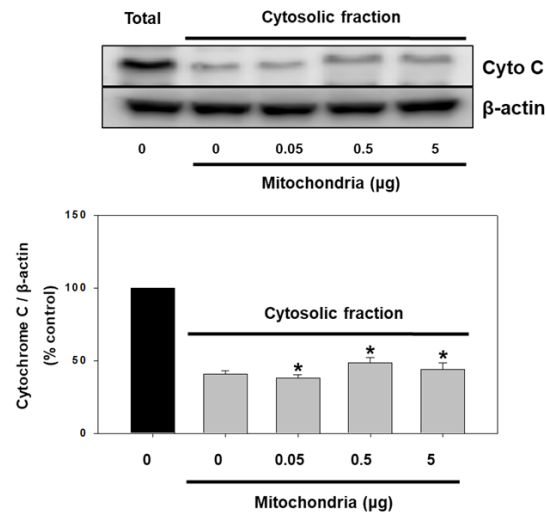
B.



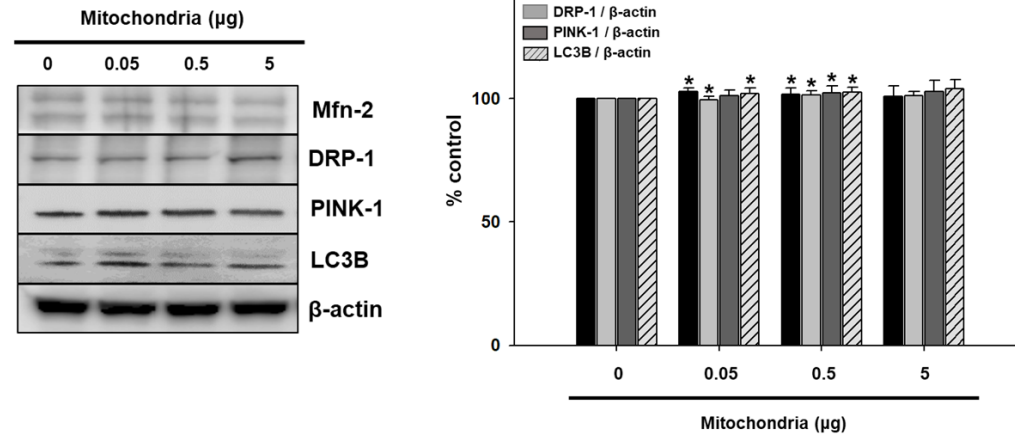
C.



D.

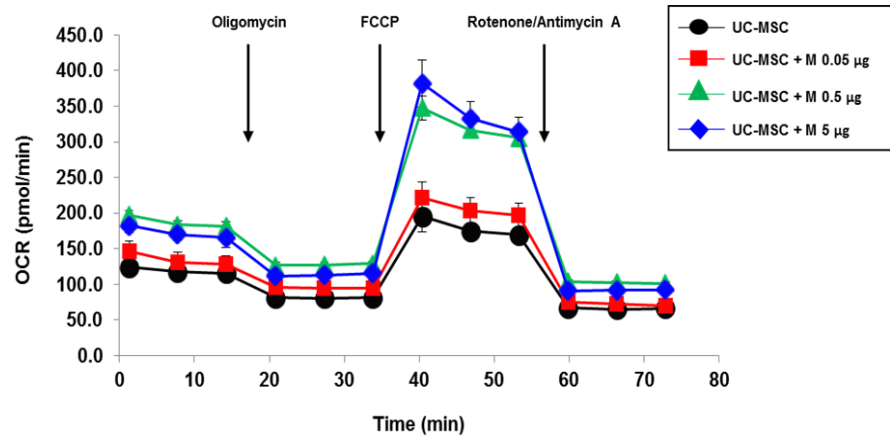


E.

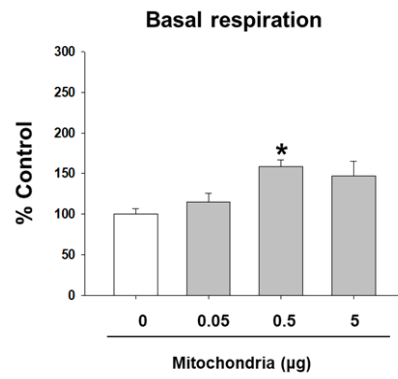


Supplementary Figure S3 (Continued on next page).

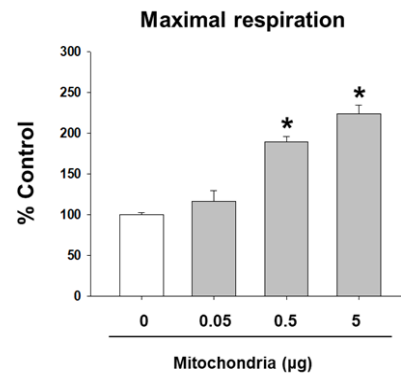
F.



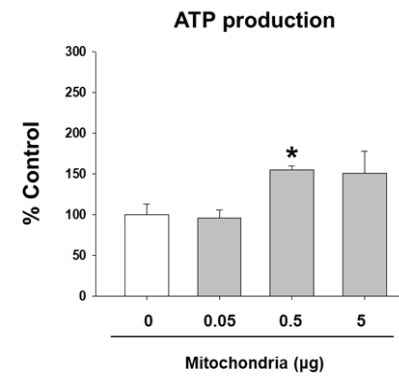
G.



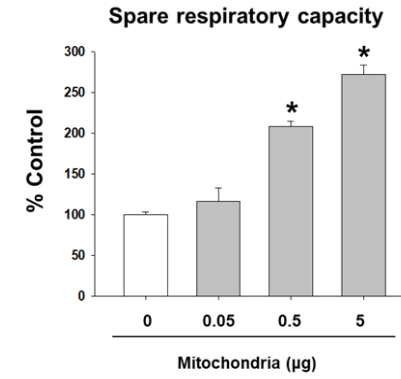
H.



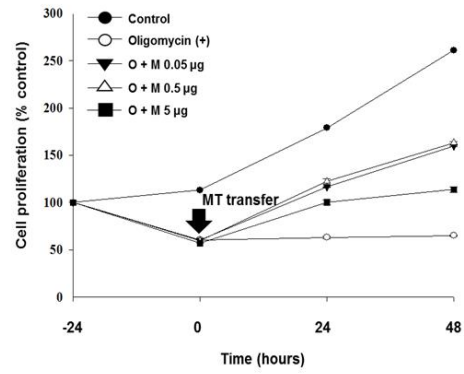
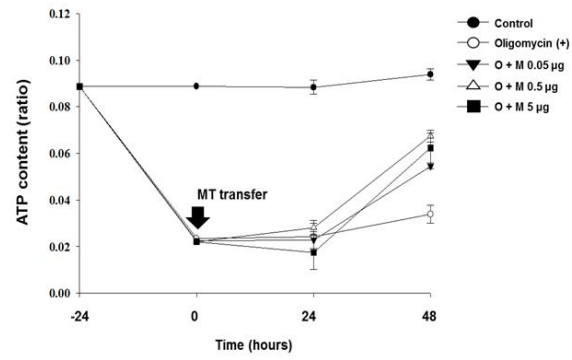
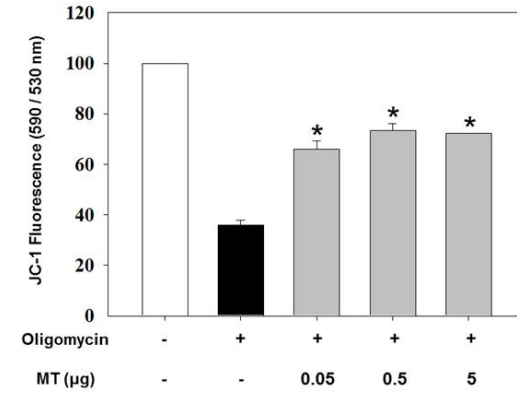
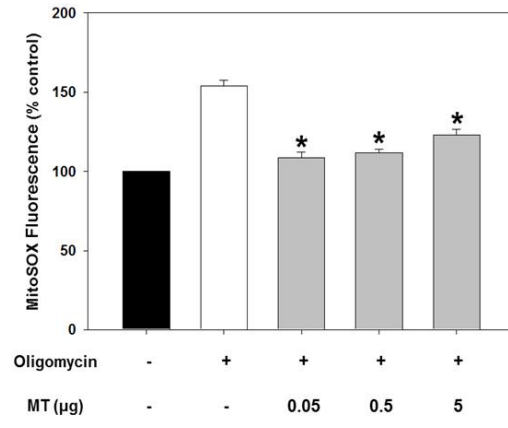
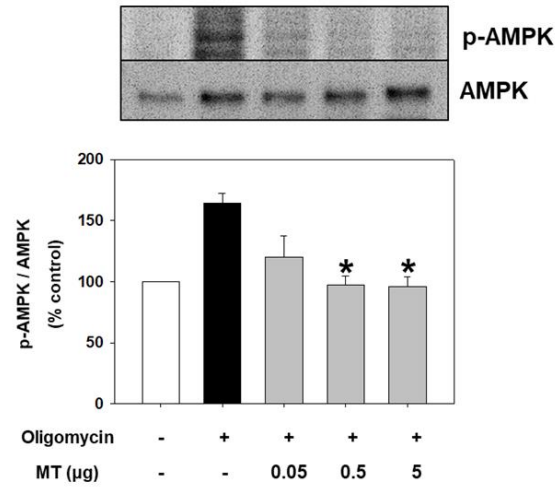
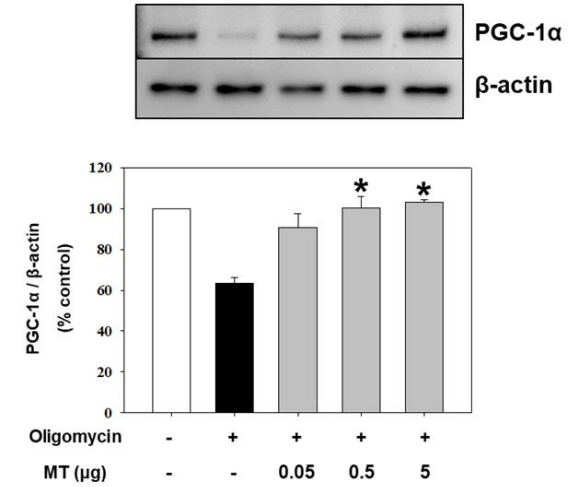
I.

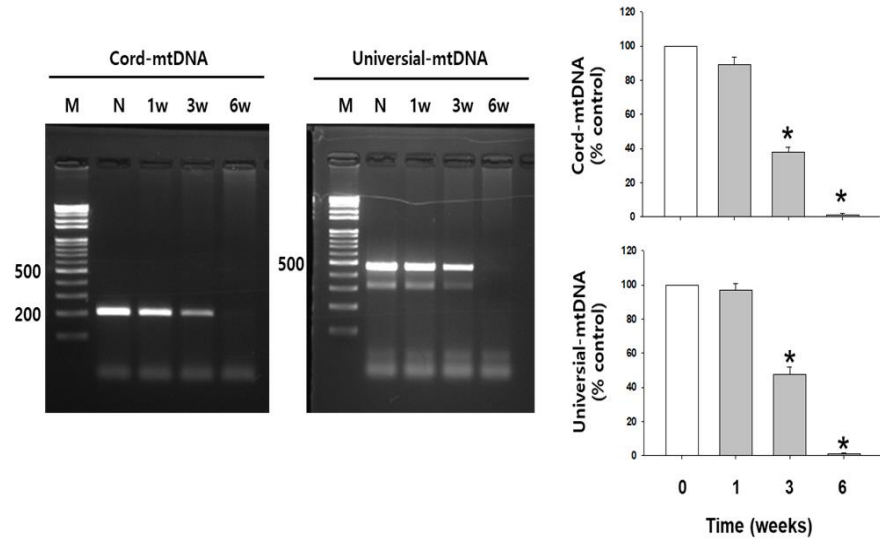
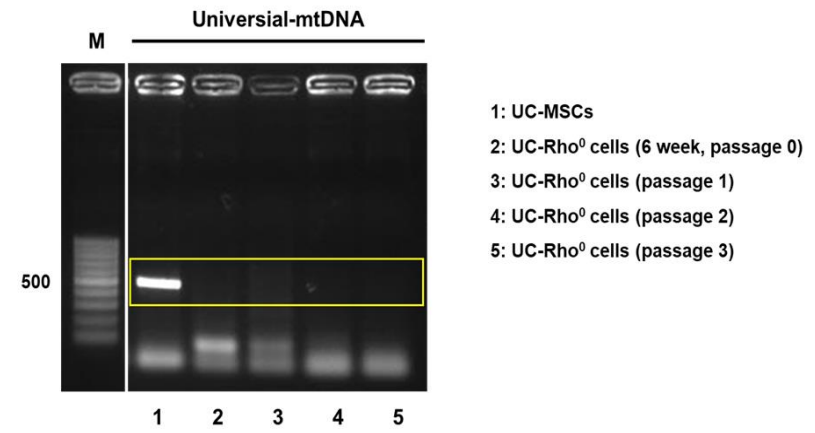
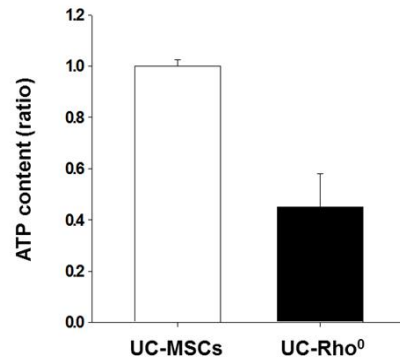
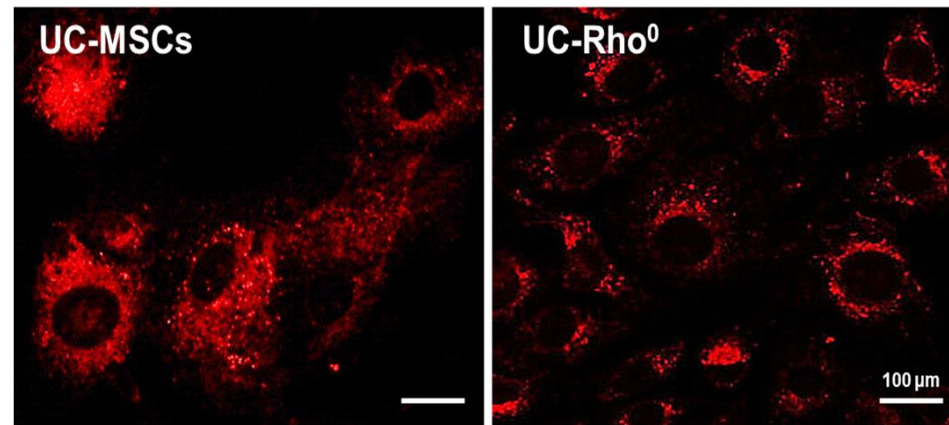


J.

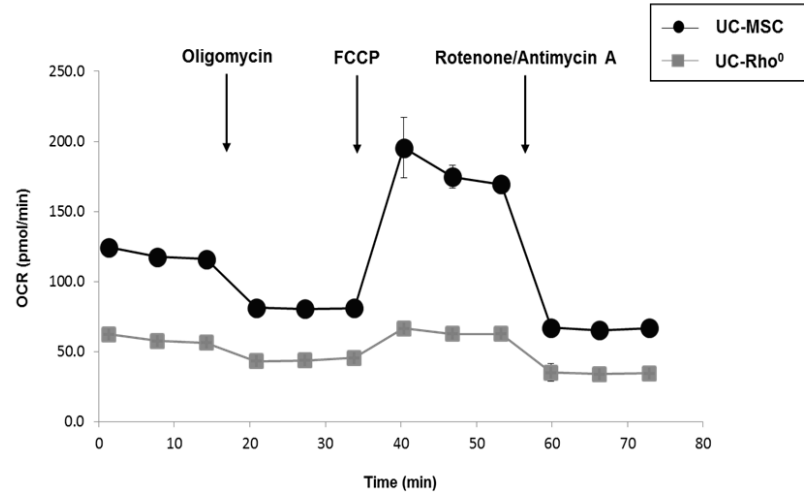


Supplementary Figure S3 (continued).

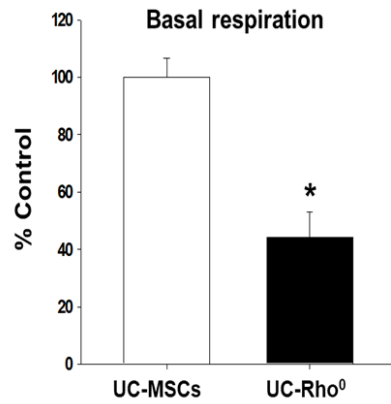
A.**B.****C.****D.****E.****F.**

A.**B.****C.****D.**

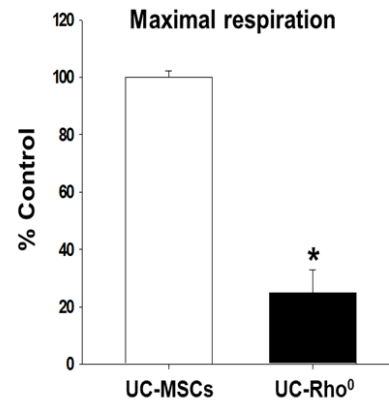
E.



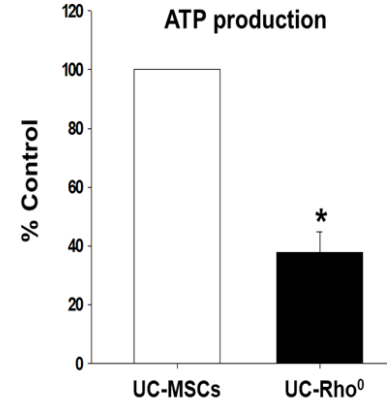
F.



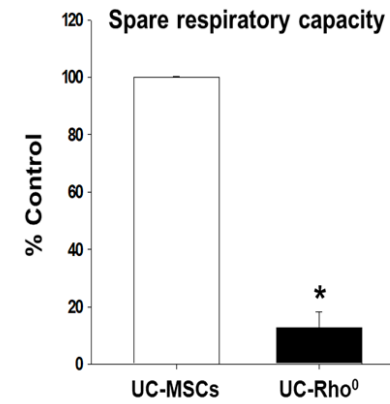
G.



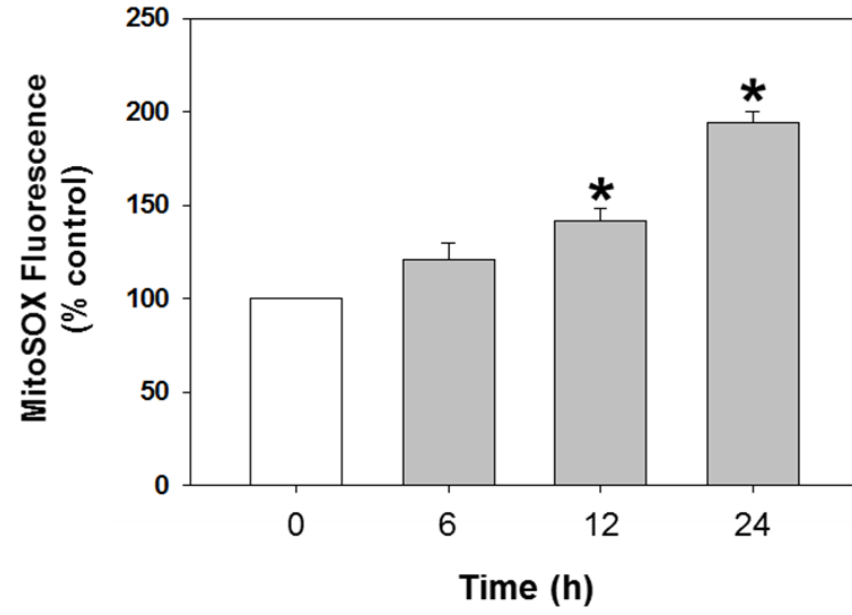
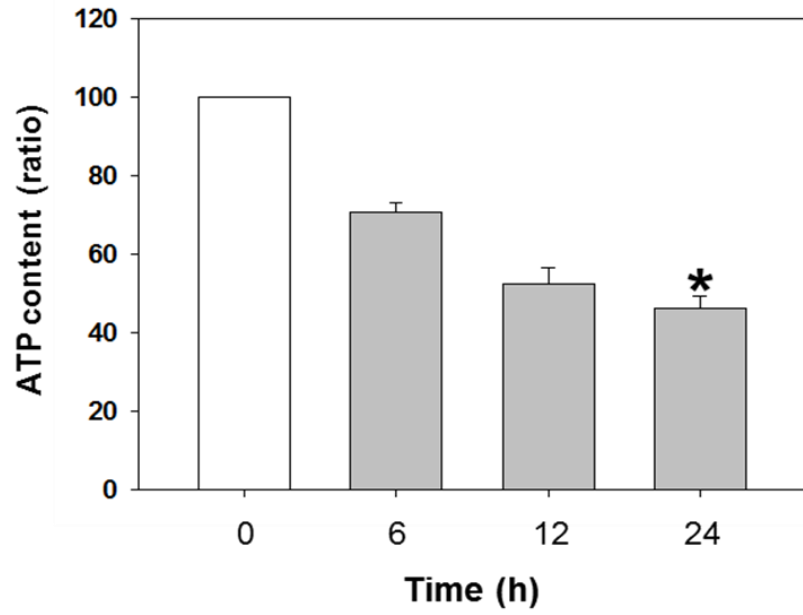
H.



I.



Supplementary Figure S5 (Continued).



Supplementary Figure S6

158

159

160 **Supplementary Figure S7**
161 **Full length image of results by Western blot analysis**

Fig. 3E

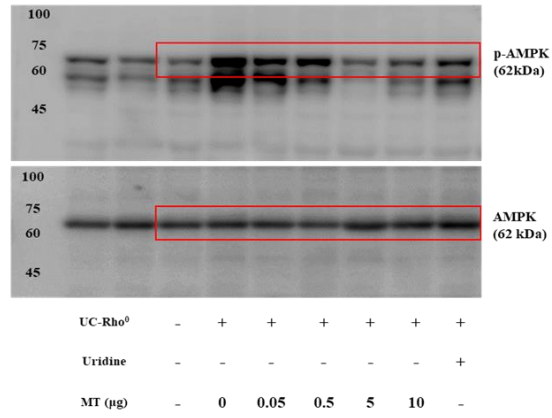


Fig. 3F

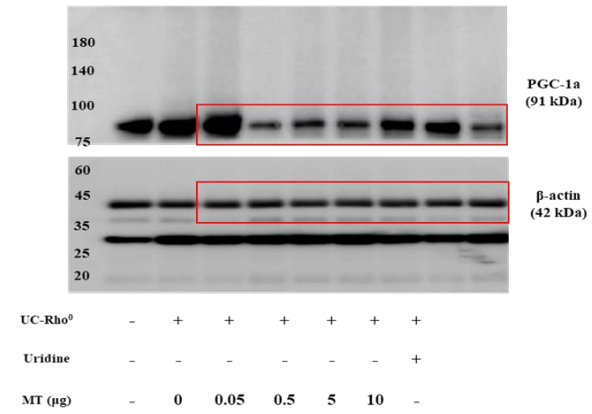


Fig. 4D

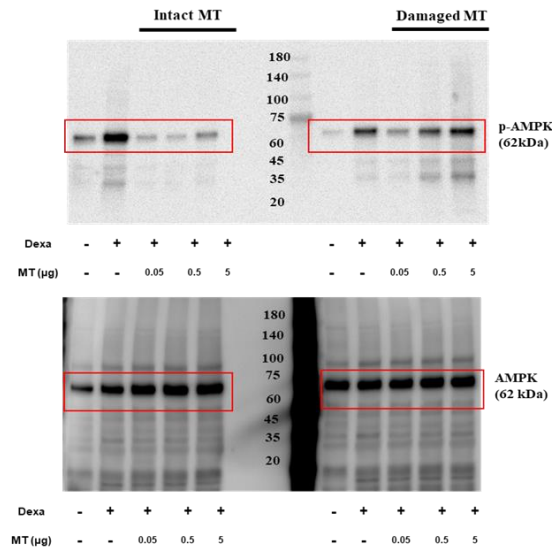


Fig. 4E

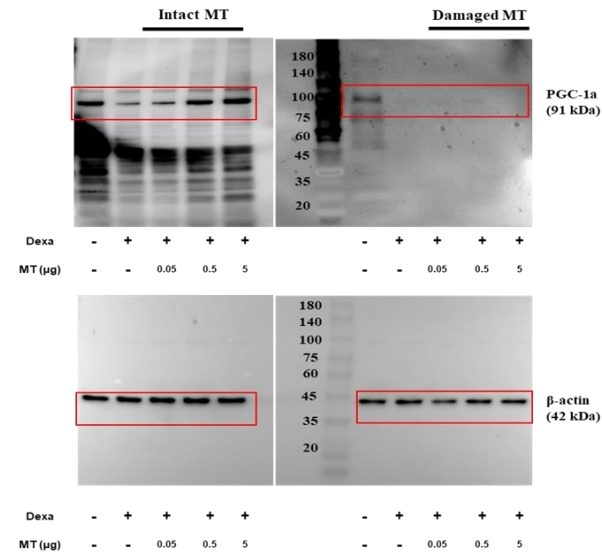


Fig. 4F

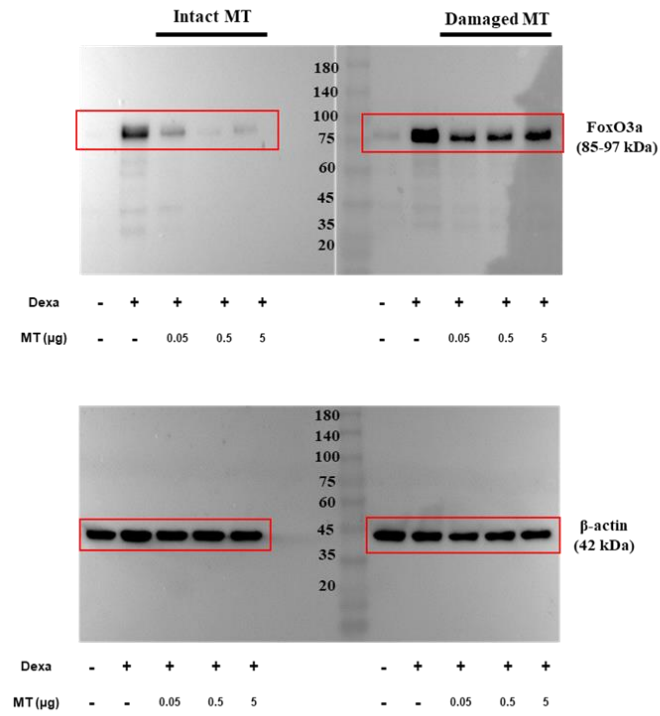
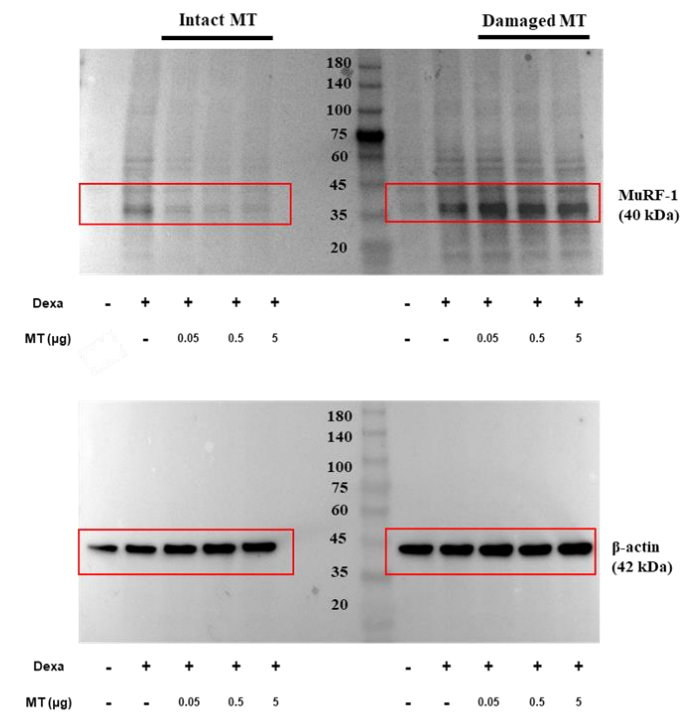


Fig. 4G



Supplementary Figure S7 (Continued on next page).

Fig. S1E

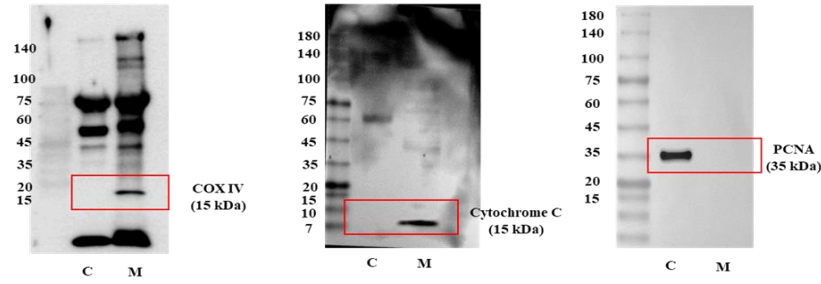


Fig. S3D

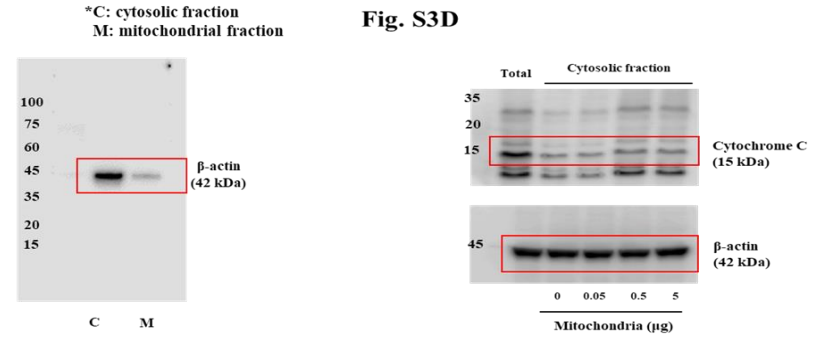


Fig. S3E

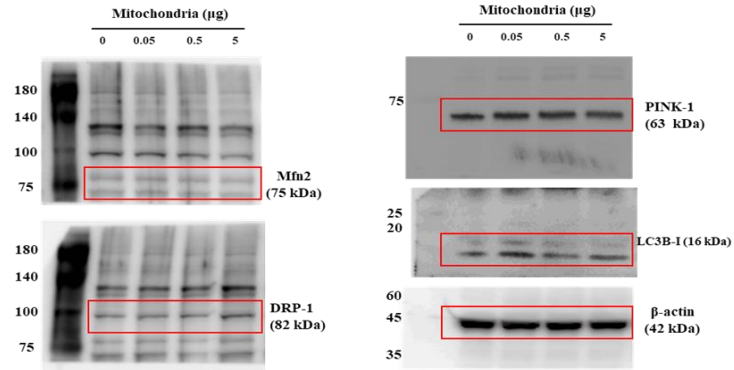


Fig. S4E

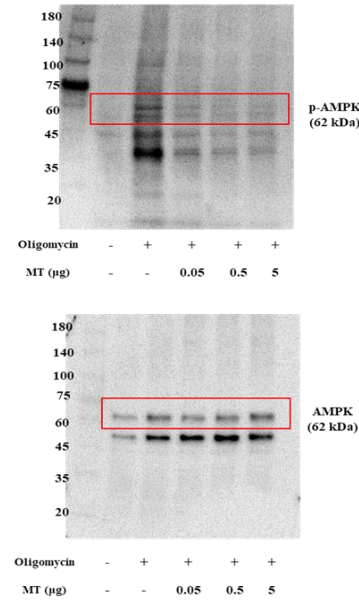
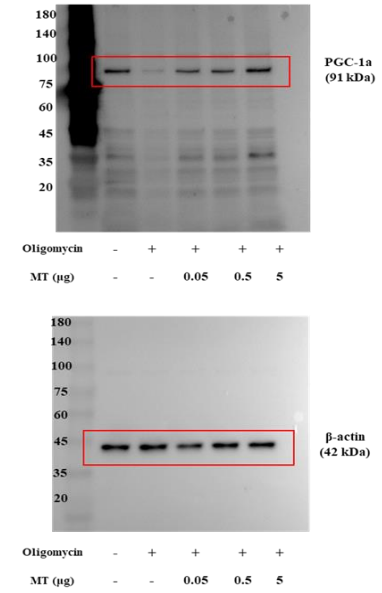


Fig. S4F



165 **Supplementary References**

166

- 167 1. Kalyanaraman, B *et al.* Measuring reactive oxygen and nitrogen species with fluorescent probes: challenges and limitations. *Free radic. Biol. Med.*
168 **52**, 1-6, doi:10.1016/j.freeradbiomed.2011.09.030 (2012).
- 169 2. Yang, J. *et al.* Prevention of apoptosis by Bcl-2: release of cytochrome c from mitochondria blocked. *Science* **275**, 1129-1132 (1997).
- 170 3. Gottlieb, E., Armour, S. M., Harris, M. H. & Thompson, C. B. Mitochondrial membrane potential regulates matrix configuration and cytochrome c
171 release during apoptosis. *Cell death Differ.* **10**, 709-717 (2003).
- 172 4. Peng, K. *et al.* Resveratrol Regulates Mitochondrial Biogenesis and Fission/Fusion to Attenuate Rotenone-Induced Neurotoxicity. *Oxid. Med. Cell.*
173 *Longev.* **2016**, 6705621, doi:10.1155/2016/6705621 (2016).